Biol. Cybern. 69, 129–137 (1993)

Biological Cybernetics

Reduction of a channel-based model for a stomatogastric ganglion LP neuron

David Golomb [1], John Guckenheimer [2], Shay Gueron [3]

[1] Laboratory of Atomic and Solid State Physics, Cornell University, Ithaca, NY 14853, USA
[2] Mathematics Department and Center for Applied Mathematics, Cornell University, Ithaca, NY 14853, USA
[3] Center for Applied Mathematics, Cornell University, Ithaca, NY 14853, USA

Received: 18 August 1992/Accepted: 30 November 1992

Abstract. Buchholtz et al. constructed a detailed conductance-based model of the LP cell of the stomatogastric ganglion of crustacea based upon the experimental work of Golowasch. Their model incorporated seven ionic currents and had 13 dynamical variables. We have produced a simplification of this model that has a seven-dimensional phase space by using the method of equivalent potentials, suggested by Abbott and Kepler, to combine several dynamical variables with similar time scales. Analysis of the dynamics of the reference and reduced model reveals similar bifurcation diagrams and similar dynamical behavior of the individual ionic currents.

1 Introduction

Neural networks are composed of individual neurons interacting via synaptic and electrical interactions. For better understanding and simpler analysis of network models, models of each neuron should be as simple as possible while retaining essential biological features. Investigations of single neurons (e.g., Tuckwell 1988; Hodgkin and Huxley 1952; Golowasch 1990; Buchholtz et al. 1992) have revealed complex behavior that depends on the properties of the neuron's ionic channels. Thus, it is important to find methods of simplifying conductance-based neuron models, which will enable us to understand better the dynamics of single neurons and neural networks.

Hodgkin and Huxley (1952) developed the first conductance-based model for a neural system. This model of the squid giant axon includes four dynamical variables: the membrane potential V, the activation variables of the sodium conductance m and of the potassium conductance n, and the inactivation variable of the sodium conductance h. Since then, several reduced models have been proposed. Fitzhugh (1961) and Nagumo (1962) proposed a two-dimensional phenomenological model which is a crude approximation of the Hodgkin–Huxley model. Its variables were the membrane potential and a slow recovery variable. Krinskii and Kokoz (1973) and Rinzel (1985) used two assumptions, that the fast variable m was an instantaneous function of V and that a linear combination of the slower variables h and n remained approximately constant during the time evolution, in proposing two-dimensional models. This technique of finding numerical relationships between several variables and using them for dimension reduction was used by Rose and Hindmarsh (1989) also. They reduced six- and seven-dimensional thalamic neuron models to one with three dynamical variables. Abbott and Kepler (1990) introduced a more systematic reduction method that was further analyzed by Kepler et al. (1992) and by Meunier (1992). They reduced the Hodgkin–Huxley model to a two-dimensional system by using the instantaneous m approximation and combining the variables h and n, which have a similar time scale. Their method, called the method of *equivalent potentials*, is discussed in the following section. A six-dimensional model which adds an A-current I_A to the Hodgkin–Huxley model was reduced to a three-dimensional one by Kepler et al (1992), by introducing three time scales: the fast one of V and m, the slower one of h, n and a_A (the activation variable of I_A) and the slowest one of b_A (the inactivation variable of I_A).

Golowasch (Golowasch 1990; Buchholtz et al. 1992) created a detailed conductance-based model for the **LP** neuron of the stomatogastric ganglion (STG) of the rock crab *Cancer borealis*. This 13-dimensional model is described in Sect. 2. We have produced a seven-dimensional model that yields similar dynamical behavior. In Sect. 3, we discuss the properties of a "good" reduced model and describe the reductions we make to the 13-dimensional model. In Sect. 4 the two

Correspondence to: D. Golomb

models are compared, with an emphasis upon the parameter dependence of observed dynamical behavior. The results are summarized in Sect. 5.

2 The reference model for the LP cell

2.1 The structure of the model

The mathematical model of Golowasch (1990) and Buchholtz et al. (1992) for the LP cell (with some small changes) was used as the starting point for our work. This dynamical system is a single-compartment model which consists of a set of coupled differential equations, and can be regarded as an extension of the Hodgkin–Huxley model with additional currents taken into account. In the following, we give a brief description of this model, which we refer to as the *reference model.*

The change in the electrical potential of the model neuron is caused by the accumulation of currents that flow through channels located within the membrane and an external current injected through an electrode. The cell is assumed to be isopotential with its membrane potential V, satisfying the equation:

$$C_m \frac{dV}{dt} = I_{ext} - \sum_j I_j , \tag{1}$$

where C_m is the membrane capacitance and the currents I_j are the ionic currents that flow through the membrane. Each of the ionic currents is represented by

$$I_j = \bar{g}_j a^p b^q (V - E_j) , \tag{2}$$

where E_j is the reversal potential of the jth current, a and b are activation and inactivation variables, and p and q are integers. The $\bar{g}_j$ represents the "maximum" conductance corresponding to activated channels with no inactivation. Note that some channels never approach such a fully activated state. The dynamics of the activation variables are described by differential equations:

$$\frac{da_j}{dt} = k_j(V)[a_{j\infty}(V) - a_j] , \tag{3}$$

where $a_{j\infty}$ and k_j are the (voltage-dependent) steady-state value and the relaxation rate of the process, respectively. For the calcium-activated current, they also depend on the calcium concentration. The activation steady-state values are represented by a sigmoidal function with half-maximum potential (i.e., the voltage where $a_{j\infty}$ attains the value $\frac{1}{2}$) V_j and width s_j:

$$a_{j\infty}(V) = \{1 + \exp[(V - V_j)/s_j]\}^{-1} . \tag{4}$$

The dynamics of the inactivation variables are modelled analogously.

The different currents that flow through the membrane are as follows (Golowasch 1990; Golowasch and Marder 1992; Buchholtz et al. 1992):

I_{ext} is an external current (e.g., experimentally injected current).

I_{Na} is the sodium current. This current is strongly voltage dependent and is largely responsible for generating action potentials. It is represented by a fast activation variable (m) and an inactivation variable (h). The associated maximal conductance is $\bar{g}_{Na}$.

I_d is the delayed rectifier potassium current. This current is responsible for the brief hyperpolarization at the end of an action potential. It has no significant inactivation and thus it is represented by its activation variable (n) and its maximal conductance $\bar{g}_d$ alone.

$I_{0(Ca)}$ is the calcium-activated potassium current. It is represented by a voltage and calcium dependent activation (a_0) and inactivation (b_0) variables, and a maximal conductance $\bar{g}_0$.

I_A is the transient A-like current. It is a transient potassium outward current that flows following a period of hyperpolarization. It is represented by an activation variable (a_A), an inactivation variable (b_A) and maximal conductance $\bar{g}_A$.

I_{Ca} is the calcium current. This current is both voltage and calcium dependent, and it is represented by a combination of activation (a_{Ca1}, a_{Ca2}) and inactivation (b_{Ca1}) voltage- and calcium-dependent variables. The associated maximal conductances are $\bar{g}_{Ca1}$ and $\bar{g}_{Ca2}$, respectively.

I_h is a hyperpolarization-activated inward (h) current. It is controlled by a single activation process (r) and the associated maximal conductance is $\bar{g}_h$.

I_l is the leak current. Since it is not voltage dependent in our model, it is represented by its constant maximal conductance (g_l).

2.2 The equations of the reference LP cell model

The reference (LP cell) model consists of 13 differential equations. Equation (5) is for the membrane potential V. Equation (6) represents the calcium ATPase mechanism, where $[Ca]$ is the calcium concentration. Equations (7)–(17) govern the dynamics of the activation and inactivation variables. The different currents appear in the right-hand side of (5), which is a detailed version of (1). The parameters of the model are presented in Table 1.

$$\begin{aligned} C_m \frac{dV}{dt} = I_{ext} &- \underbrace{\bar{g}_{Na} m^3 h (V - E_{Na})}_{I_{Na}} - \underbrace{\bar{g}_d n^4 (V - E_K)}_{I_d} \\ &- \underbrace{\bar{g}_0 a_0 b_0 (V - E_K)}_{I_{0(Ca)}} - \underbrace{\bar{g}_A a_A^3 b_A (V - E_k)}_{I_A} \\ &- \underbrace{(\bar{g}_{Ca1} a_{Ca1} b_{Ca1} + \bar{g}_{Ca2} a_{Ca2})(V - E_{Ca})}_{I_{Ca}} \\ &- \underbrace{\bar{g}_h r (V - E_h)}_{I_h} - \underbrace{\bar{g}_l (V - E_l)}_{I_l} , \end{aligned} \tag{5}$$

$$\frac{d}{dt}[Ca] = -c_{iCa} I_{Ca} - k_{Ca}([Ca] - [Ca^0]) , \tag{6}$$

$$\dot{m} = k_m(a_m(V) + b_m(V))(m_\infty(V) - m) , \tag{7}$$

$$\dot{h} = k_h(a_h(V) + b_h(V))(h_\infty(V) - h) , \tag{8}$$

$$\dot{n} = k_n(V)(n_\infty(V) - n) , \tag{9}$$

Table 1. Parameters used in the model

Current	Maximum conductance (μS)	Reversal potential (mV)	Rate constant (s^{-1})	Half-maximum potential (mV)	Width (mV)	Other parameters
Delayed rectifier (I_d)	$\bar{g}_d = 0.35$	$E_k = -80$	$c_n = 180$	$V_n = -25$ $V_{kn} = 10$	$s_n = -17$ $s_{kn} = -22$	
Calcium-activated outward current (I_{Ca})	$\bar{g}_{oCa} = 3.2$	$E_k = -80$	$k_{oa} = 600$ $k_{ob} = 35$ $k_{Ca} = 360$	$V_{ao1} = 0$ $V_{ao2} = -16$	$s_{ao1} = -23$ $s_{ao2} = -5$	$f = 0.6$ mV/μM $c_1 = 2.5$ μM $c_2 = 0.7$ μM $c_3 = 0.65$ μM $[Ca^0] = 0.05$ μM $c_{iCa} = 300$ μM/nC
A-current (I_A)	$\bar{g}_A = 1.7$	$E_k = -80$	$k_A = 140$ $k_B = 20$	$V_A = -12$ $V_B = -70$	$s_A = -26$ $s_B = 6$	
Ca^{2+} current (I_{oCa})	$\bar{g}_{Ca1} = 0.21$ $\bar{g}_{Ca2} = 0.047$	E_{Ca} [a]	$k_{aCa1} = 50$ $k_{bCa1} = 16$ $k_{aCa2} = 10$	$V_{aCa1} = -11$ $V_{bCa1} = -50$ $V_{aCa2} = 22$	$s_{aCa1} = -7$ $s_{bCa1} = 8$ $s_{aCa2} = -7$	
Inward rectifier (I_h)	$\bar{g}_h = 0.037$	$E_h = -10$	$c_r = 0.33$	$V_r = -60$ $V_{kr} = -110$	$s_r = 7$ $s_{kr} = -13$	
Fast Na^+ (I_{Na})	$\bar{g}_{Na} = 2300$	$E_{Na} = 50$	$k_m = 10000$ $k_h = 500$	$V_{am} = -6$ $V_{bm} = -34$ $V_{ah} = -39$ $V_{bh} = -40$	$s_{am} = -20$ $s_{bm} = -13$ $s_{ah} = -8$ $s_{bh} = -5$	$c_{am} = 0.11$ mV^{-1} $c_{bm} = 15$ $c_{ah} = 0.08$
Leak current (I_l)	$\bar{g}_l = 0.1$	$E_l = -50$				$C_m = 1.7$ nF

[a] $E_{Ca} = 115.5 - 12.2 \ln[Ca]$

$$\dot{a}_0 = k_{0a}(a_{0\infty}(V, [Ca]) - a_0), \tag{10}$$

$$\dot{b}_0 = k_{0b}(b_{0\infty}([Ca]) - b_0), \tag{11}$$

$$\dot{a}_A = k_A(a_{A\infty}(V) - a_A), \tag{12}$$

$$\dot{b}_A = k_B(b_{A\infty}(V) - b_A), \tag{13}$$

$$\dot{a}_{Ca1} = k_{aCa1}(a_{Ca1\infty}(V) - a_{Ca1}), \tag{14}$$

$$\dot{b}_{Ca1} = k_{bCa1}(b_{Ca1\infty}(V) - b_{Ca1}), \tag{15}$$

$$\dot{a}_{Ca2} = k_{aCa2}(a_{Ca2\infty}(V) - a_{Ca2}), \tag{16}$$

$$\dot{r} = k_r(V)(r_\infty(V) - r). \tag{17}$$

The sigmoid function $H(V, \tilde{V}, \tilde{S})$, defined as

$$H(V, \tilde{V}, \tilde{S}) = (1 + e^{(V-\tilde{V})/\tilde{S}})^{-1}, \tag{18}$$

is useful for defining the rate constants and the steady-state values of the parameters. The voltage-dependent rate constants are

$$k_n(V) = c_n H(V, V_{kn}, S_{kn}), \tag{19}$$

$$k_r(V) = c_r H(V, V_{kr}, S_{kr}). \tag{20}$$

The steady-state values for the activation and inactivation variables are given by:

$$m_\infty = a_m(V)/(a_m(V) + b_m(V)), \tag{21}$$

$$a_m(V) = c_{am}(V + V_{am}) \frac{1}{1 - \exp\left(\frac{V - V_{am}}{S_{am}}\right)}, \tag{22}$$

$$b_m(V) = c_{bm} \exp\left(\frac{V - V_{bm}}{S_{bm}}\right), \tag{23}$$

$$h_\infty(V) = a_h(V)/(a_h(V) + b_h(V)), \tag{24}$$

$$a_h(V) = c_{ah} \exp\left(\frac{V - V_{ah}}{S_{ah}}\right), \tag{25}$$

$$b_h(V) = H(V, V_{bh}, S_{bh}), \tag{26}$$

$$n_\infty(V) = H(V, V_n, S_n), \tag{27}$$

$$a_{0\infty}(V, [Ca]) = H(V, V_{a01} - f[Ca], S_{a01}) \times H(V, V_{a02} - f[Ca], S_{a02}) \frac{[Ca]}{c_1 + [Ca]}, \tag{28}$$

$$b_{0\infty}([Ca]) = \frac{c_2}{c_3 + [Ca]}, \tag{29}$$

$$a_{A\infty}(V) = H(V, V_A, S_A), \tag{30}$$

$$b_{A\infty}(V) = H(V, V_B, S_B), \tag{31}$$

$$a_{Ca1\infty}(V) = H(V, V_{aCa1}, S_{aCa1}), \tag{32}$$

$$b_{Ca1\infty}(V) = H(V, V_{bCa1}, S_{bCa1}), \tag{33}$$

$$a_{Ca2\infty}(V) = H(V, V_{aCa2}, S_{aCa2}), \tag{34}$$

$$r_\infty(V) = H(V, V_r, S_r). \tag{35}$$

This version of the LP cell model is different from the original Golowasch model in the following details:

1. There is only one inactivation parameter b_A for the A-current. Its half maximal potential is $V_B = -70$ mV, the width of the sigmoid curve is $S_B = 6$ mV and its rate constant is $k_B = 20\ s^{-1}$. The conductance $\bar{g}_a$ is set to be 1.7 μS. This form of the A-current fits better the experimental results for the spiny lobster *Panulirus interruptus* (R. M. Harris-Warrick 1992, personal communication), while the original

model of Golowasch et al. (Golowasch 1990; Buchholtz et al. 1992) was developed for the rock crab *Cancer borealis*.

2. For the same reason, the half maximal potential of the h current is set to be $V_r = -60$ mV.

3. The parameter c_3 in (29) which defines the (voltage and calcium dependent) steady-state value b_0 was set to be 0.65 μM instead of 0.6 μM. This change was necessary in order to prevent $b_{0\infty}$ from being larger than 1 at small calcium concentrations, and has no considerable effect on the dynamics.

3 Reduction of complex cellular models

3.1 Properties of good reduction

The dynamics of ionic-conductance cell models are described by a multidimensional dynamical system and can sometimes be very complex. However, in the case of the reference model, trajectories appear to have a simple asymptotic behavior within the biologically interesting parameter regime, either tending to an equilibrium point or a limit cycle. We seek a representation of the dynamics of the model by a set of coupled differential equations with fewer dynamical variables, i.e., with a lower-dimensional phase space. It is easier to calculate the bifurcation scheme of such a reduced model, and it can be seen as a first step in a chain of approximation that will simplify the complex reference model.

An ideal reduction scheme is the one which produces the same dynamics as the reference model for equivalent parameter values. Insofar as our reduction preserves the set of ionic currents in the reference model, we would like these currents to be similar in the two models. In terms of the function of the neuron within a network, only the temporal behavior of $V(t)$ is important because this is the only variable which is responsible for interactions among neurons. Hence, from this point of view, an ideal reduced model should have the same solutions, $V(t)$, as the solution of the original one for comparable parameter values and initial conditions. In relating the two models, there should be no change in the membrane potential $V(t)$. Unfortunately, it is usually impossible to find such a reduced model, and we formulate weaker requirements for a "good" reduction scheme.

Throughout this paper, a good reduction scheme is a scheme which yields a reduced model with the following properties. It is assumed that the parameters which define the reduced model functions of the parameters which define the reference model. Hence, the effect of changing parameters of the reference model can be tested in both models.

1. The reduced model has the same qualitative behaviors as the reference model. For example, if the reference model can show quiescent, tonic or bursting behavior, depending on its parameters, the reduced model should do the same.

2. The regions yielding different types of dynamical behavior in the reference model are mapped to the regions with the same types of behavior by the functions which relate the parameters of the reduced model to those of the reference model. In particular, the bifurcation sets that form the boundaries of these regions are mapped to each other by the functions which map parameters of the reference model to parameters of the reduced model.

3. Within corresponding regions of the parameter spaces, the dynamic behaviors of the reference and reduced model are similar. In the quiescent regime, the steady-state voltages should be the same. In the periodic regime, the amplitudes and frequencies of the function $V(t)$ should be the same for equivalent points in parameter spaces. Hence, a change in the parameter values due to external input or the neurotransmitters will yield the same change in the dynamics. In a bursting regime, the reduced model should also present the same number of action potentials per burst.

A "good" reduced model should satisfy all these criteria at least in the parameter regime which is biologically interesting.

3.2 LP model reduction using the method of equivalent potentials

Abbott and Kepler (1990) proposed a systematic strategy, the method of *equivalent potentials*, for the reduction of a reference model (Kepler et al. 1992; Meunier 1992). In cases where the steady-state values of activation or inactivation variables are monotonic functions of the membrane potential, these variables can be converted to equivalent potentials U_j defined by the equation

$$a_j = a_{j\infty}(U_j)\,, \tag{36}$$

i.e., $U_j = a_{j\infty}^{-1}(a_j)$. Here $a_{j\infty}^{-1}$ denotes the inverse function of $a_{j\infty}$. The equations of motion, expressed by the equivalent potentials, are

$$\frac{\mathrm{d}U_j}{\mathrm{d}t} = \frac{k_j(V)}{a'_{j\infty}(U_j)}\left[a_{j\infty}(V) - a_{j\infty}(U_j)\right], \tag{37}$$

where the prime means differentiation with respect to the argument. If several "equivalent potentials" U_j behave in a similar way under different conditions, a good approximation is to combine them together and represent them by one variable. A necessary condition for this grouping of variables is that their dynamics have similar time scales, i.e., the rate constants are close. This method of combining several equivalent potentials into one is not unique. Several methods are described by Abbott and Kepler (1990), Kepler et al. (1992), and Meunier (1992), based on the relative contribution of the various variables to the dynamics of the membrane potential. We examine here the application of these methods to the reference model of the LP cell described in Sect. 2.

The equivalent potentials for activation and inactivation variables, together with the membrane potential, are presented in Fig. 1. The input current is taken to be

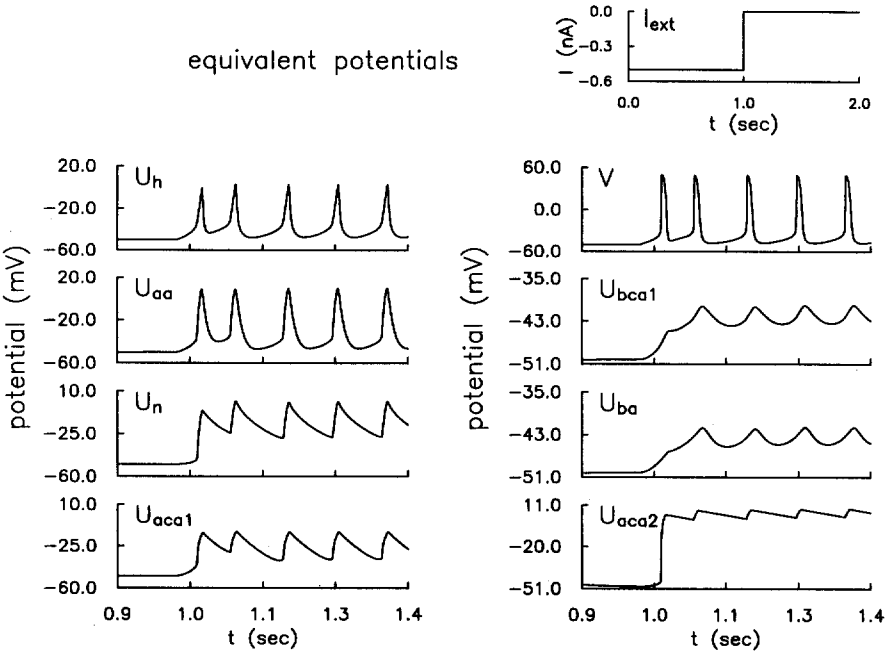

Fig. 1. The time evolution of the membrane potential V and the equivalent potential of activation and inactivation variables. An external current $I_{ext} = -0.5$ nA is injected into the neuron for 1 s. Then, at $t = 1.0$ s, I_{ext} is set to zero. Similarity is seen between the dynamical behavior of U_h and U_{aa}, U_n and U_{aca1}, and U_{bca1} and U_{ba}

$I_{ext} = -0.5nA$ for 1 s, during which the system converges to equilibrium. Then, it is set instantaneously to zero and the neuron starts firing. The equivalent potentials have the same period as the membrane potential, but their amplitude is smaller. In general, an equivalent potential which corresponds to a slower variable will have a smaller amplitude. Two equivalent potentials are considered as similar if their minimal and maximal values and their rise and fall times are close. Similarity is seen between U_h and U_{aa} and between U_{ba} and U_{bca1}. The trajectories of U_n and U_{aca1} have similar shapes, but the value of U_{aca1} is smaller. The trajectory of U_{aca2} looks different than those of the other slow variables, U_{bca1} and U_{ba}. The reason for this is that the half-maximum potential of a_{ca2}, 22 mV, is much higher than those of b_{ca1} and b_A, and when there is no action potential a_{ca2} is small. The rate of change of an activation variable is proportional to the difference between its current value and its steady state value. When the action potential is created, a_{ca2} increases rapidly, but still remains small. When the action potential ends, a_{ca2} decays slowly. This behavior is not shared by the other variables.

We have grouped the variables according to the similarities of their dynamics:

1. The sodium activation variable m, whose time scale is much faster than all the other activation and inactivation variables, is considered as instantaneous: $m(t) = m_\infty(V(t))$.

2. The activation of the A-current, a_A, is taken as a function of U_h, the "equivalent potential" of the sodium inactivation variable: $a_A(t) = a_{A\infty}(U_h(t))$. The activation of the calcium-activated potassium current, a_o, is taken as a function of U_h and the instantaneous value of the calcium concentration $a_o(t) = a_{0\infty}(U_h, [Ca])$. Using U_h is justified in both cases because the rate constants of these currents, $k_A = 140$ and $k_{oa} = 600$, have the same order of magnitude as $k_h = 500$. Taking the concentration of a_o as an instantaneous function of the calcium concentration is a good approximation because the dynamics of a_o is faster than that of the calcium concentration itself.

3. The dynamical behavior of the reference model in the $U_n - U_{aca1}$ plane is plotted in Fig. 2 for the stimulus shown in Fig. 1. During the time when the neuron fires tonically, the curve is close to a straight line. We used the approximation $U_{aca1} = 0.91U_n - 11$ mV, shown in Fig. 2. In contrast to the pure method of equivalent potentials, this approximation causes the equilibrium voltage of the reduced model to deviate from that of the reference model, but it is a good approximation when the neuron fires tonically.

4. The inactivation variables of the A-current, b_A, and of the first calcium current, b_{ca1}, have similar time scales ($k_B = 20$ and $k_{bca1} = 16$) and half-maximum voltage of their steady-state value. Hence, the approximation $b_A = b_{A\infty}(U_{bca1})$ has been used.

5. The activation variable of the h-current is much slower than all the other variables. Thus, it was held constant and regarded as a parameter. The value $r = 0.1$ has been chosen.

The dynamical variables have been divided into groups depending on the time-scale of their evolution. For simplicity, the dynamics of the "combined" variable is governed by the equation of motion of the most important variable in the group, i.e., the variable which

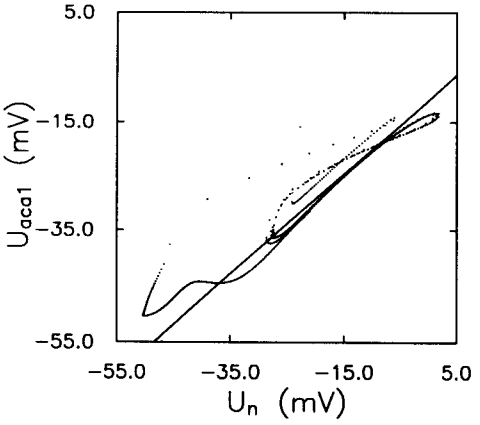

Fig. 2. The trajectory of the neuron in the U_n–U_{aca1} plane for the current stimulus shown in Fig. 1. The *straight line* is the approximate reltinoship between the two variables in the tonic regime

contributes the most to changes in $V(t)$. These variables are U_h, U_n and U_{bca1}. We have observed that the methods described by Abbott and Kepler (1990), Kepler et al. (1992) and Meunier (1992) and our methods give similar results if it is possible to combine several variables together. However, strict adherence to their methods yields a more complex model than the one described here. In contrast to the case of the Hodgkin–Huxley model, we have not succeeded in combining the variables h and n, and in this model they belong to two different groups. The reason that they remain separate is that the time constant of h is in the order of 500, while k_n is much smaller, especially at low voltages. The inactivation variable of the calcium-activated potassium current, b_o, depends only on the calcium concentration, but its dynamics is slow, so it remains a separate variable.

The reduced model has seven parameters (V, $[Ca]$, U_h, U_n, U_{bca1}, a_{ca2} and b_o) instead of 13. The equations defining the reduced model are the following:

$$\begin{aligned} C_m \frac{dV}{dt} = I_{ext} &- \underbrace{\bar{g}_{Na} m_\infty^3(V) h_\infty(U_h)(V - E_{Na})}_{I_{Na}} \\ &- \underbrace{\bar{g}_d n_\infty^4(U_n)(V - E_K)}_{I_d} \\ &- \underbrace{\bar{g}_0 a_{0\infty}(U_h, [Ca]) b_0 (V - E_K)}_{I_{0(Ca)}} \\ &- \underbrace{\bar{g}_A a_{A\infty}^3(U_h) b_{A\infty}(U_{bca1})(V - E_K)}_{I_A}, \\ &- \underbrace{(\bar{g}_{Ca1} A_{Ca1\infty}(0.91 U_n - 11) b_{Ca1\infty}(U_{bca1}) + \bar{g}_{Ca2} a_{Ca2})(V - E_{Ca})}_{I_{Ca}} \\ &- \underbrace{0.1\bar{g}_h(V - E_h)}_{I_h} - \underbrace{\bar{g}_l(V - E_l)}_{I_l} \end{aligned} \tag{38}$$

$$\dot{U}_h = k_h \frac{(a_h(V) + b_h(V))(h_\infty(V) - h_\infty(U_h))}{\frac{\partial}{\partial U_h}\frac{a_h(U_h)}{a_h(U_h) + b_h(U_h)}}, \tag{39}$$

$$\dot{U}_n = k_n(V) \frac{n_\infty(V) - n_\infty(U_n)}{H'(V, V_n, S_n)}, \tag{40}$$

$$\dot{U}_{bca1} = k_{bCa1} \frac{b_{Ca1\infty}(V) - b_{Ca1\infty}(U_{bca1})}{H'(V, V_{bCa1}, S_{bCa1})}, \tag{41}$$

together with (6), (11), (16) and (18–34). The parameters in Table 1 are still to be used. The function $H'(V, \tilde{V}, \tilde{S})$ is defined to be:

$$H'(V, \tilde{V}, \tilde{S}) = \frac{\partial H(V, \tilde{V}, \tilde{S})}{\partial V}. \tag{42}$$

4 Comparison between the reduced and reference models

In the parameter regimes that have been examined, the trajectories obtained from both the reference and the reduced model either converge to an equilibrium point or to a limit cycle (tonic firing). Usually, there appears to be only one attractor. However, there is a regime of bistability where the equilibrium point and the limit cycle coexist.

To assess the quality of the reduced model, we compared it with the reference model according to the criteria of Sect. 3. Since the models include a large number of parameters, we concentrated on regions of parameter space which are biologically interesting. For both the reference and the reduced model, the values of parameters are those listed in Table 1, except for $\bar{g}_{Na}$ which has varied in our study. The variations in the behavior of both models with respect to the parameters I_{ext} and $\bar{g}_{Na}$ are depicted in a bifurcation diagram showing the transitions between different types of behavior. The external current represents the response of the neuron to external stimuli, while the sodium conductance was chosen as a second parameter to vary because of the importance of the sodium current in the creation of action potentials. In both models, three regions are seen. At low values of I_{ext}, the neuron is quiescent. Then, at a certain value I_{ext}^1 of I_{ext}, a limit cycle corresponding to tonic firing of action potentials starts to coexist with the equilibrium, i.e., the state is bistable. At a second value I_{ext}^2 of I_{ext}, the equilibrium loses stability or ceases to exist, and the limit cycle is the only stable attractor. As seen in Fig. 3, the critical currents at which bifurcations occur decrease when $\bar{g}_{Na}$ increases. The bifurcation curves of the reduced model are close to those of the reference one. There are two main differences between the models:

1. In the refererence model, the equilibrium point loses its stability via a subcritical Hopf bifurcation (Guckenheimer and Holmes 1983), while in the reduced model it disappears via a saddle-node bifurcation. The behavior of the limit cycle is unrelated to the local properties of the bifurcation in both cases. The constant r approximation is responsible for this change of the

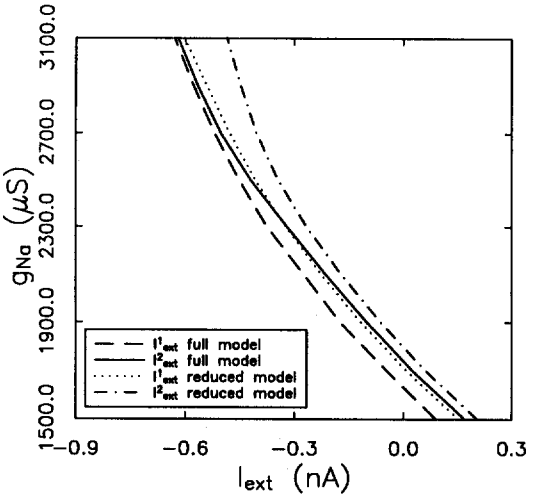

Fig. 3. The bifurcation diagram of the reference and reduced models. For the reference model, the equilibrium becomes unstable at I^2_{ext} (*reference line*), while the stable periodic trajectory starts to exist at I^1_{ext} (*dashed line*). For the reduced model, the equilibrium points disappeared at I^2_{ext} (*dashed-dotted line*), while the stable periodic trajectory starts to exist at I^1_{ext} (*dotted line*)

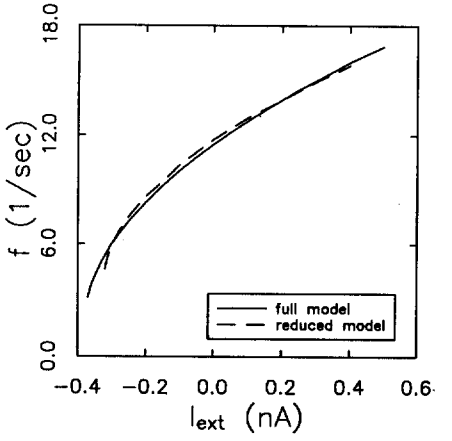

Fig. 4. The frequency of tonic firing versus external current for the reference model (*continuous curve*) and reduced model (*dashed curve*)

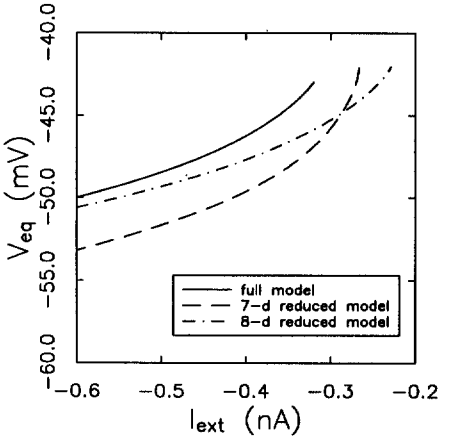

Fig. 5. The equilibrium voltage for the reference model (*continuous curve*) and the seven-dimensional reduced model (*dashed curve*). The *dashed-dotted* line represents the equilibrium potential for an eight-dimensional reduced model which includes r as a variable

bifurcation type. A model which leaves r as a dynamical variable but includes all the other approximations of the reduced model has Hopf bifurcations. The very slow variable r is responsible for very slow unstable oscillations, and treating it as a constant parameter eliminates them and changes the bifurcation type. For example, when $\bar{g}_{Na} = 2300$ μS, $I^2_{ext} = -0.32$ nA and the time period of the Hopf bifurcation is 1.47 s.

2. The range of I_{ext} in the bistable regime decreases as a function of $\bar{g}_{Na}$ in the reference model but increases in the reduced one. Again, the constant r approximation is the main source of this discrepancy. The value of r in the reduced model, $r = 0.1$, is a good approximation for $\bar{g}_{Na} = 2300$. However, for higher values of g_{Na}, the critical external current is smaller and hence the equilibrium voltage is smaller too. Thus, in the bifurcation region the value of r is larger in the reduced model than in the reference model, and the approximation is less accurate.

For comparing the dynamical behavior of the models, the oscillation frequency was calculated versus the external current. As shown in Fig. 4, the two curves are very similar. The main difference occurs in the region near the bifurcation.

The equilibrium voltage of the two models versus I_{ext} is presented in Fig. 5. The voltage of the reduced model is lower by about 3 mV. This difference was caused by the approximation of U_{acal} as a function of U_n and by the constant r assumption. In order to investigate the relative effect of the approximations on the equilibrium potential, we plotted the equilibrium potential obtained from an eight-dimensional model which leaves r as a dynamical variable. As shown in Fig. 5, the approximation of constant r causes a larger effect at lower values of I_{ext}, while the effect of approximating U_{acal} as a function of U_n is more important at higher values of I_{ext}, where it is closer to the bifurcation. For typical neural models, we speculate that this discrepancy in equilibrium voltage is a minor effect since the primary interactions between neurons are synaptic. In situations where the shift of equilibrium voltage is important for synaptic interactions (Johnson et al. 1991), one can compensate for the effect in a network model by rescaling the dependence of the synaptic conductance on the voltage of the presynaptic neuron.

The general character of the oscillations of the reduced model is similar to those of the reference model. Since both models included the same set of ionic currents, they could be compared directly. The contribution of each current has been calculated for both models, and Fig. 6 presents the comparison. The results from the two models were almost identical.

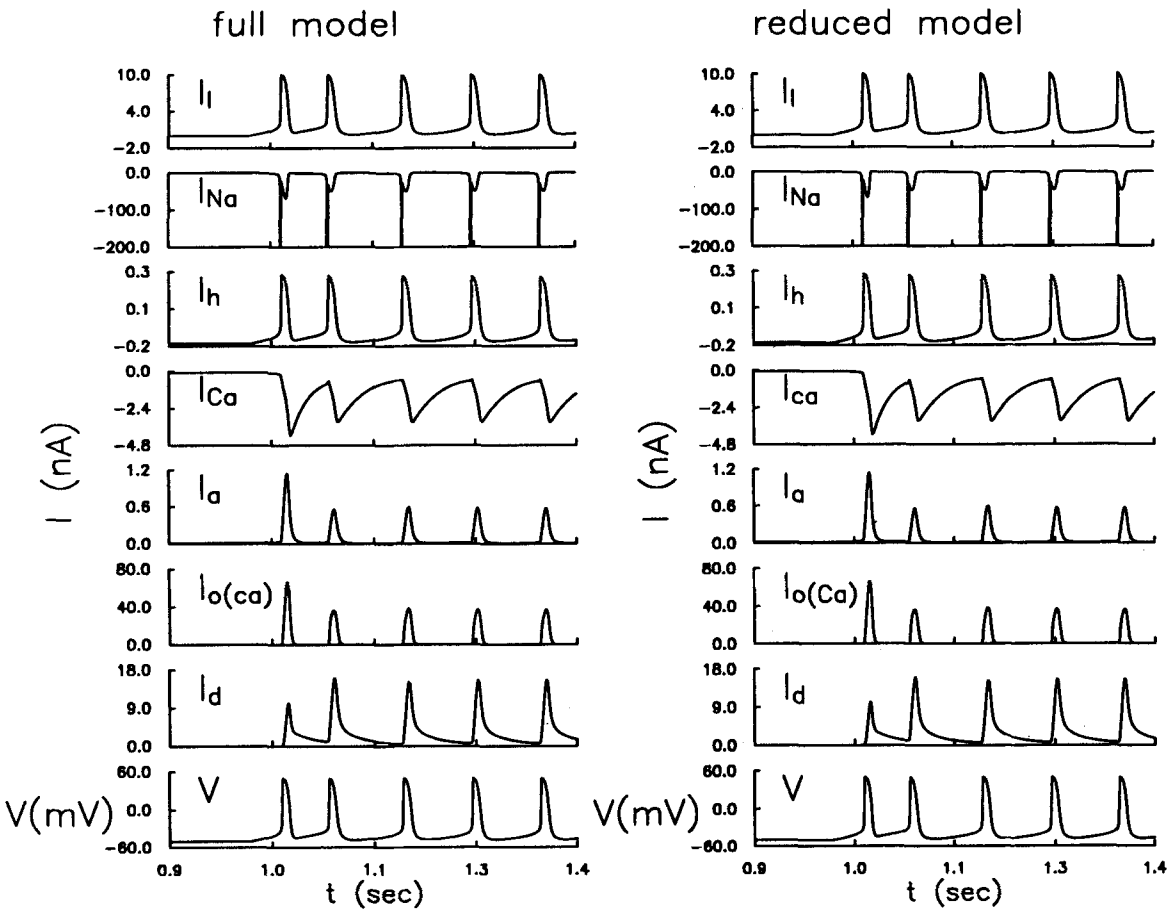

Fig. 6. The evolution of the ionic current for the injection of a step current described in Fig. 1. The results from the reference and the reduced model are almost identical

5 Summary and discussion

Our version of the Golowasch model of the LP cell is a single-compartment conductance-based model that incorporates several kinds of ionic channel, each of which is represented by an activation (and sometimes an inactivation) variable. By combining variables whose temporal behavior is strongly correlated throughout the parameter regions we have explored, the number of dynamical variables (i.e., the dimension of the phase space) was reduced from 13 to seven. Two of these seven variables are the membrane voltage and the calcium concentration, and three represent dynamics of activation and inactivation on different time scales. A sixth variable, a_{ca2}, has a time scale which is comparable with those of two other variables in the reference model, but it cannot be combined with them because it has a half-maximum voltage (22 mV) which is much larger than the half-maximum voltages of the other slow variables. Hence, it increases relatively fast when there is an action potential and decays slowly afterwards. This behavior is different from the behavior of the other slow variables. The steady-state value of the seventh variable, b_0, depends only on the calcium concentration.

The reduced model was tested according to the criteria defined for a "good" reduction scheme. These criteria are more stringent than those formulated by previous authors in that we demand that the model retain information about the parameter values at which bifurcations between different types of asymptotic dynamics occur. The models examined here have similar types of limiting behavior: equilibrium, tonic firing and an intermediate regime of bistability. The parameters of the reduced model are the same parameters as those of the reference model. Therefore, the parameter regions of the two models were compared. In the bifurcation diagram, the boundaries separating the different dynamical regimes are close.

The various time scales of the LP neuron can be viewed as various levels of integration over the "history" of the neuron. They should be included in the reduced model in order to enable it to respond to different kinds of stimuli in the same way the reference model responds. In this work we have eliminated the slowest time scale of the reference model, corresponding to the variable r, by treating it as a constant parameter. Since the time scale of r is larger than the time period of the firing, this approximation is relatively good for most purposes. In a better approximation r may be

taken as a function of parameters (like $\bar{g}_{Na}$), and in this way the similarity between the bifurcation diagrams of the reference and reduced models can be improved. However, eliminating other time scales in the model, which are comparable to or shorter than the firing frequency, causes large differences in the behavior of reduced models.

Acknowledgments. The research of David Golomb and Shay Gueron was partially supported by Rothschild Fellowships and that of John Guckenheimer by the National Science Foundation. We thank Ronald Harris-Warrick for his helpful comments, Mark Myers for his assistance with the calculations of the bifurcation curves in the models, and Eve Marder, Larry Abbott and Jorge Golowasch for sharing their work (upon which ours is based) prior to publication. The software package dstool (Back et al. 1992) was used for the numerical studies that form the basis of this paper.

References

Abbott LF, Kepler TB (1990) Model neurons: from Hodgkin–Huxley to Hopfield. In: Garridol (ed) Statistical mechanics of neural networks. Springer, Berlin Heidelberg New York

Back A, Guckenheimer J, Myers M, Wicklin F, Worfolk P (1992) dstool: computer assisted exploration of dynamical systems. Not Am Math Soc 39:303–309

Buchholtz F, Golowasch J, Epstein IR, Marder E (1992) Mathematical model of an identified stomatogastric ganglion neuron. J Neurophysiol 67:332–340

Fitzhugh R (1961) Impulses and physiological stages in theoretical models of nerve membrane. Biophys J 1:445–466

Golowasch J (1990) Characterization of a stomatogastric ganglion neuron. A biophysical and a mathematical description. PhD dissertation, Brandeis University, Waltham, Mass

Golowasch J, Marder E (1992) Ionic currents of the lateral pyloric neuron of the stomatogastric ganglion of the crab. J Neurophysiol 67:318–331

Guckenheimer J, Holmes P (1983), Nonlinear oscillations, dynamical systems, and bifurcation of vector fields. Springer, Berlin Heidelberg New York

Guckenheimer J, Gueron S, Harris-Warrick RM (1993) The dynamics of conditionally bursting neuron. Proc R Soc Lond (Biol) in press

Hodgkin AL, Huxley AF (1952) Measurement of current-voltage relations in the membrane of the giant axon of the *Loligo*. J Physiol (Lond) 117:500–544

Johnson BR, Peck JH, Harris-Warrick RM (1991) Temperature sensitivity of graded synaptic transmission in the lobster stomatogastric ganglion. J exp Biol 156:267–285

Kepler TB, Abbott LF, Marder E (1992) Reduction of conductance-based neuron models. Biol Cybern 66:381–387

Krinskii VI and Kokoz YM (1973) Analysis of equations of excitable membranes. 1. Reduction of the Hodgkin–Huxley equations to a second-order system. Biofizika 18:506–511

Meunier C (1992) Two and three dimensional reductions of the Hodgkin–Huxley system: separation of time scales and bifurcation schemes. Biol Cybern 67:461–468

Nagumo JS, Arimito S, Yoshizawa S (1962) An active pulse transmission line simulating nerve axon. Proc IRE 50:2061–2070

Rinzel J (1985) Excitation dynamics: insights from simplified membrane models. Fed Proc 44:2944–2946

Rose RM, Hindmarsh JL (1989) The assembly of ionic currents in a thalamic neuron. I. three-dimensional model. Proc R Soc Lond (Biol) 237:267–288

Tuckwell HC (1988) Introduction to theoretical biology. Cambridge University Press, Cambridge